Bioorganic & Medicinal Chemistry 20 (2012) 6904–6918

Contents lists available at SciVerse ScienceDirect

Bioorganic & Medicinal Chemistry

journal homepage: www.elsevier.com/locate/bmc

G-quadruplex DNA cleavage preference and identification of a perylene diimide G-quadruplex photocleavage agent using a rapid fluorescent assay

Michelle Schoonover [a], Sean M. Kerwin [a,b,*]

[a] Department of Chemistry and Biochemistry, University of Texas at Austin, Austin, TX 78712, USA
[b] Division of Medicinal Chemistry, College of Pharmacy, University of Texas at Austin, Austin, TX 78712, USA

ARTICLE INFO

Article history:
Received 16 August 2012
Revised 10 October 2012
Accepted 18 October 2012
Available online 27 October 2012

Keywords:
Photocleavage
Porphyrins
c-Myc promoter
G-quadruplex DNA
Perylene diimide

ABSTRACT

A rapid fluorescence assay for G-quadruplex DNA cleavage was used to investigate the preference of TMPyP4 photochemical and Mn·TMPyP4 oxidative cleavage. Both agents most efficiently cleave the c-Myc promoter G-quadruplex. Direct PAGE analysis of selected assay samples showed that for a given cleavage agent, different cleavage products are formed from different G-quadruplex structures. Cleavage assays carried out in the presence of excess competitor nucleic acid structures revealed the binding selectivity of cleavage agents, while comparisons with duplex cleavage efficiency employing a dual-labeled hairpin oligonucleotide revealed neither agent prefers G-quadruplex over duplex substrates. Finally, this assay was used to identify the perylene diimide Tel11 as a photocleavage agent for the c-Myc G-quadruplex.

1. Introduction

Guanosine-rich DNA sequences can form stable secondary structures known as G-quadruplexes, the building blocks of which are tetrads made of four hydrogen bonded guanine bases (G-tetrads).[1] G-quadruplexes are highly polymorphic structures, adopting multiple molecularities and topologies based on both DNA sequence and environmental factors.[2,3] There is a growing interest in understanding the dynamic nature and potential biological roles of G-quadruplex structures in vivo.[4,5] Many DNA sequences with the potential to form these structures have been identified, including telomeric repeats,[6] various oncogene promoters,[7–9] and fragile sites associated with genomic rearrangement.[10,11] Evidence that these structures have biological roles also comes from the identification of enzymes that recognize and process G-quadruplexes[12–14] including nucleases that cleave G-quadruplex DNA.[15,16]

Recent proposals for a role of G-quadruplex structures as 'sinks' for oxidative DNA damage[17] has led to an increased interest in studies of the potential roles of G-quadruplex structures in oxidative telomere shortening and cleavage.[18] There are conflicting reports of the relative propensity of duplex versus G-quadruplex DNA to undergo oxidative attack and cleavage, and for electron 'hole' transport through duplex-G-quadruplex junctions.[19–22] It is becoming clear, however, that the topology of G-quadruplex structures may play an important role in these processes.[23]

A small number of organic and coordination compounds have been shown to cleave G-quadruplex DNA;[19,21,22,24–27] however, many of these are also known to cleave duplex DNA. Some of these G-quadruplex cleavage agents have been used as molecular probes in vitro, specifically as tools to distinguish G-quadruplex folding molecularities and topologies.[28–30] However, to date only relatively lengthy PAGE-based assays have been employed to characterize these G-quadruplex cleavage agents, and issues of selectivity for different G-quadruplex structures or for a given G-quadruplex versus duplex DNA or other higher-order DNA structures have not been addressed.

In light of the structural diversity of G-quadruplex DNA, we reason that different G-quadruplex DNA structures may have distinct susceptibilities to cleavage, depending upon the nature of the cleavage agent. Understanding these preferences is important if these agents are to be used as probes for G-quadruplex structures in a biological setting. Equally important is establishing the selectivity of G-quadruplex cleavage agents for these structures versus duplex and other, higher-order DNA structures. Given the limited number and relatively low selectivity of known G-quadruplex cleavage agents, there is a need to identify new, more selective agents for potential use as biological probes.

In this work we employ a rapid solution fluorescence assay[31] to characterize the relative efficiency of G-quadruplex cleavage of two model cleavage agents on different G-quadruplex structures. Further insights into the nature of the G-quadruplex cleavage products was obtained by direct PAGE analysis of selected assay samples. The solution based assay was used to determine the effect

* Corresponding author. Tel.: +1 512 471 5074; fax: +1 512 232 2606.
E-mail address: skerwin@austin.utexas.edu (S.M. Kerwin).

0968-0896/$ - see front matter © 2012 Elsevier Ltd. All rights reserved.
http://dx.doi.org/10.1016/j.bmc.2012.10.017

of excess competitor DNA on the G-quadruplex cleavage efficiency of these agents, in conjunction with direct measurement of duplex DNA cleavage using a 'break-light'[32] assay. Finally, the utility of the solution G-quadruplex cleavage assay for discovering new cleavage agents is demonstrated by the identification of a perylene diimide as a photocleavage agent targeting the c-Myc promoter G-quadruplex. While previous studies of G-quadruplex ligands have focused on binding selectivity, these studies demonstrate that functional selectivity, specifically preferential cleavage of G-quadruplex targets, can be accomplished with ligands that have only modest binding selectivity for G-quadruplex DNA.

2. Results and discussion

TMPyP4 and Mn(=O)TMPyP4 (Fig. 1) were selected for study as a model G-quadruplex cleavage agents. TMPyP4 is known to bind to a range of G-quadruplex structures.[33–37] The photocleavage of duplex DNA by TMPyP4 has been reported.[38,39] TMPyP4 and related porphyrins have also been reported to photocleave G-quadruplex DNA preferentially at G's associated with one or both terminal G-tetrad faces.[26,27,40,41] The oxo-metalloporphyrin Mn(=O)TMPyP4, generated in situ by oxidation of Mn·TMPyP4, has also been reported to cleave duplex[42] and G-quadruplex DNA.[29] Despite these reports of G-quadruplex cleavage with these two agents, many details concerning their cleavage selectivity for different G-quadruplex structures or G-quadruplex structures versus other nucleic acid structures remain to be addressed. It was reasoned that the rapid G-quadruplex cleavage assay employed here would be useful in addressing these issues of cleavage selectivity.

The solution fluorescence assay for G-quadruplex cleavage employed here utilizes dual-fluorescently-labeled G-quadruplex-forming oligonucleotides similar to those previously used to characterize G-quadruplex ligand binding by FRET-based G-quadruplex melting measurements[43–45] (Fig. 2). We have shown that these same oligonucleotides can be used to assay for G-quadruplex cleavage using fluorescence measurements on 96-well plates, in a manner similar to the 'break light' assay employed for screening duplex DNA-cleaving agents.[32] Briefly, in the intact G-quadruplex form, the donor FAM fluorescence emission is low due to quenching by the acceptor TAM; however, once the G-quadruplex is cleaved and the strands separate, this quenching is relieved and the FAM emission increases. In order to ensure that each cleavage event leads to disruption of the G-quadruplex, a heating/reannealing step is carried out during which only intact, intramolecular G-quadruplex structures re-form. This step is carried out after addition of a dissociation buffer to ensure that the cleavage agents are no longer bound to the DNA and that the FAM fluorescence accurately reflects the extent of cleavage.

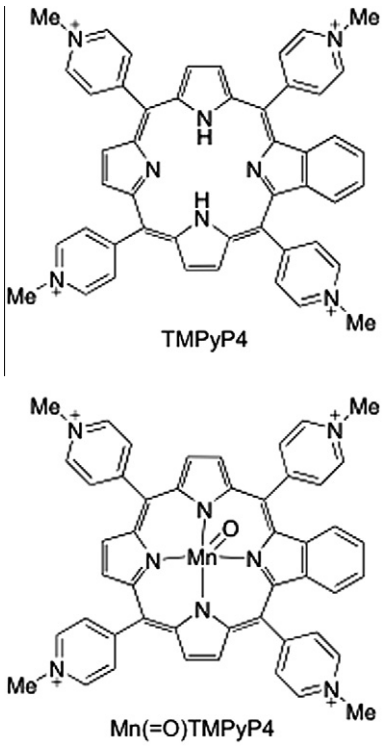

Figure 1. Structures of known photoactivated (TMPyP4) and oxidative (Mn(=O)TMPyP4) G-quadruplex cleavage ligands.

The ability of this assay to accurately measure G-quadruplex DNA cleavage has been established by comparing solution fluorescence intensities to DNA cleavage extent determined by direct PAGE electrophoresis of the assay samples[31] (also see Supplementary data, Fig. S1). It is important to note that the cleavage measured with this assay is only that which occurs spontaneously (or during the heating/reannealing step), in contrast to the majority of previous studies of G-quadruplex cleavage, which employ PAGE analysis after piperidine/heat treatment. Thus, lesions that lead to cleavage after base/heat treatment may not be detected by this assay. However, as will be shown below, these lesions can be easily detected by direct PAGE analysis of the assay samples after piperidine/heat treatment. Furthermore, the direct cleavage of G-quadruplex DNA that is measured by this assay may be more germane if the cleavage agent is to be eventually used to map G-quadruplex structure location and dynamics in a biologically relevant context.

For each cleavage agent, three G-quadruplex DNA structures were employed. Oligonucleotides containing the human telomeric sequence $(GGGTAA)_n$ are known to adopt a number of distinct topological folds.[46] In the presence of potassium ions, solution NMR studies have demonstrated to formation of a hybrid '3+1' structure (Fig. 3A).[47] In contrast, in the presence of sodium ions, an anti-parallel structure is formed (Fig. 3B).[48] The dual-labeled human telomeric G-quadruplex-forming deoxyoligonucleotide F21T consists of the human telomeric 5′-$(GGGTTA)_3GGG$-3′ sequence labeled at the 5′-end with 6-carboxyfluorescein (FAM) and at the 3′-end by tetramethylrhodamine (TAM). Similar to the corresponding unlabeled oligonucleotide, F21T adopts distinct structures in the presence of sodium versus potassium ions.[45] The nuclease hypersensitive element (NHE) III1 region of the c-MYC promoter also forms G-quadruplex structures. Although oligonucleotides comprising the wild-type sequence have been shown to form mixtures of G-quadruplex structures, a mutated sequence adopts a single G-quadruplex form, which has been characterized by NMR (Fig. 3C).[49] This parallel stranded structure is distinct from both the Na^+ and K^+ human telomeric G-quadruplexes. The dual-labeled oligonucleotide encompassing this mutated c-Myc sequence (F-c-Myc22m-T) was also employed in the cleavage studies (Fig. 3D).

2.1. Photochemical cleavage by TMPyP4

Samples of each dual-labeled G-quadruplex (250 nM) in potassium or sodium cacodylate buffer (50 mM, pH 7.4) in a 96-well plate were incubated with various concentrations of TMPyP4 for 30 min, followed by irradiation in a photoreactor fitted with lamps with a maximal emission at 420 nm. The emission of these lamps does not overlap significantly with the absorption spectra of either fluorescent label, and no significant background cleavage is observed for these dual-labeled G-quadruplexes subjected to irradiation in the absence of TMPyP4. Prior to carrying out the heating/

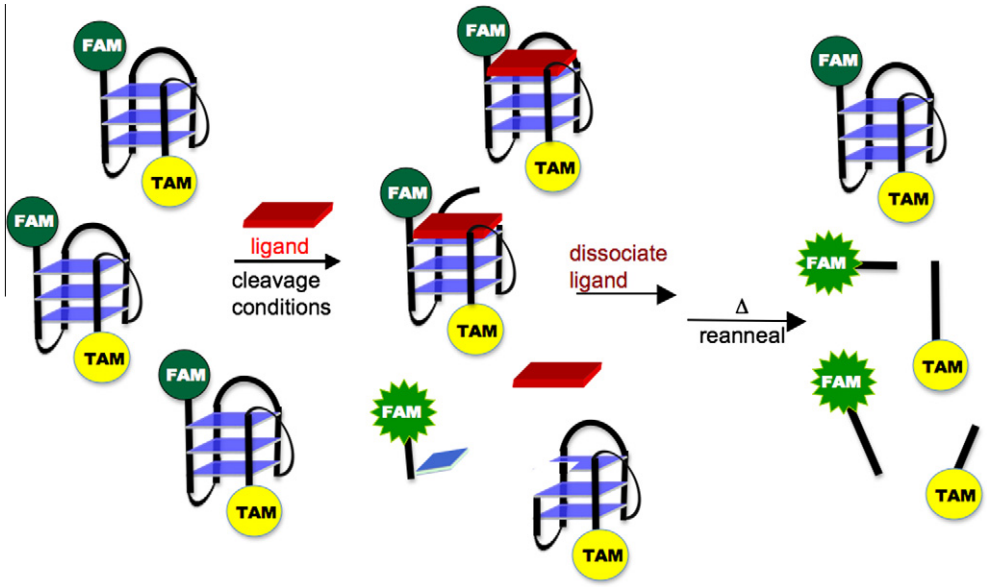

Figure 2. Design of the fluorescence G-quadruplex cleavage assay. The FAM fluorescence of a dual-labeled G-quadruplex oligonucleotide is low; however, once cleaved the fluorescence greatly increases. An immediate increase in FAM fluorescence can occur due to spontaneous nucleotide dissociation as a result of a cleavage event. Alternatively, a cleavage event that transforms the intramolecular G-quadruplex into a stable bimolecular G-quadruplex may not result in marked change in fluorescence. However, after ligand dissociation, a thermal cycle irreversibly denatures all cleaved, intermolecular G-quadruplexes, which are unlikely to reanneal at the oligonucleotide concentration (nM range) employed.

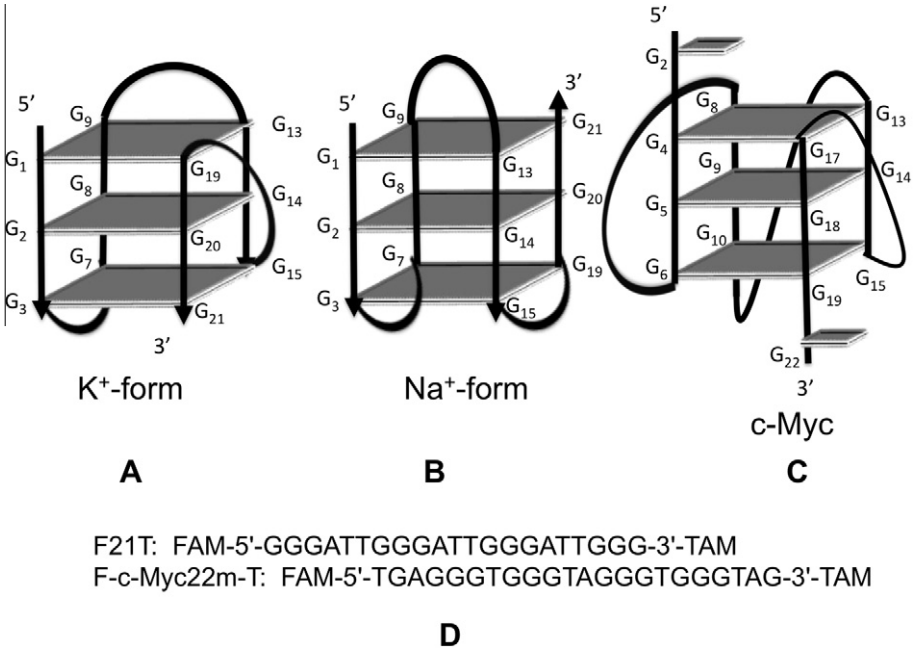

Figure 3. (A) Topology of the (3 + 1) mixed hybrid human telomeric G-quadruplex formed in the presence of potassium (K^+-form); (B) topology of the antiparallel human telomeric G-quadruplex formed in the presence of sodium (Na^+-Form); (C) topology of the parallel G-quadruplex formed by the c-Myc sequence (c-Myc); (D) sequences of the dual-labeled oligonucleotides used in this work.

reannealing step as described above, the samples were treated with a large excess of calf thymus DNA (10 μg final concentration/well) to dissociate TMPyP4 from cleaved and uncleaved G-quadruplexes (SDS can also be used, see Supplementary data, Fig. S2). The 96-well plates were sealed, heated to 85 °C for 30 min, and then allowed to slowly cool to room temperature before the FAM fluorescence was determined. To allow comparisons between runs, for each 96-well plate the fluorescence of each well was corrected for the background fluorescence due to intact G-quadruplex and TMPyP4 and normalized to a sample of G-quadruplex that had been completely cleaved by prolonged incubation with S1 nuclease (see Eq. 1 in Section 4).

These three G-quadruplex structures demonstrate distinct concentration- and irradiation time-dependent photochemical cleavage by TMPyP4. A marked increase in the FAM fluorescence was observed for K^+F21T irradiated in the presence of TMPyP4 (Fig. 4A). The fluorescence intensities of samples subjected to irradiation for 5, 10, 30 and 120 min increase proportionally with

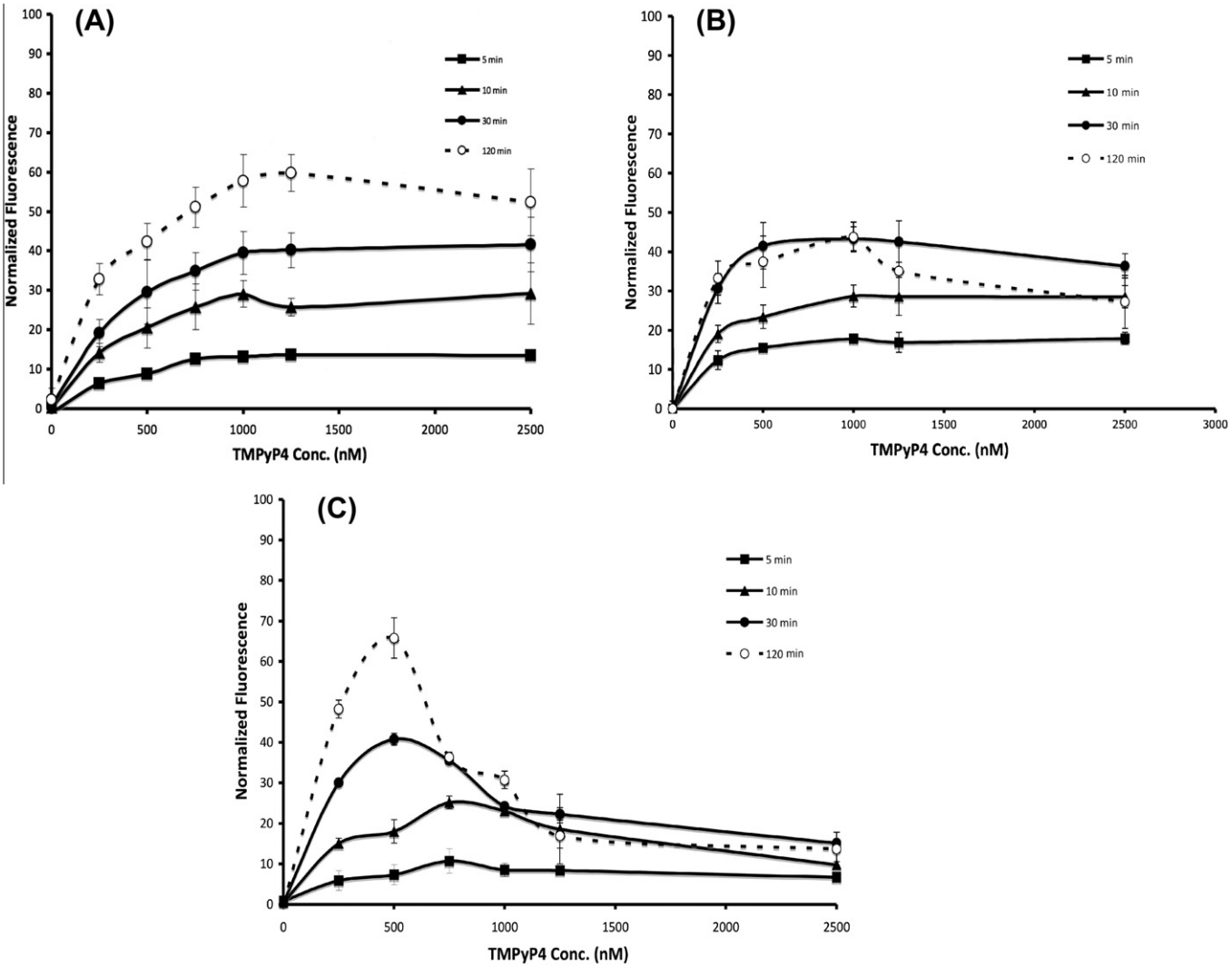

Figure 4. Normalized fluorescence intensity for different G-quadruplex DNA samples (250 nM) in the presence of 0–2.5 μM TMPyP4 irradiated (420 nm lamps) for 5–120 min. (A) K^+F21T (250 nM) in 50 mM potassium cacodylate buffer. (B) Na^+F21T (250 nM) in 50 mM sodium cacodylate buffer. (C) F-c-Myc22m-T in 50 mM potassium cacodylate buffer.

TMPyP4 concentration up to approximately 1 μM TMPyP4, or three- to fourfold excess relative to K^+F21T. At higher TMPyP4 concentrations, little further increase in fluorescence signal is noted, and at the longest irradiation time, a slight decrease in fluorescence is observed at the highest TMPyP4 concentration. The highest normalized fluorescence of ca. 60%, corresponding to cleavage of more than one-half of the K^+F21T construct initially present occurs after 120 min irradiation in the presence of 1250 nM TMPyP4.

The solution-based TMPyP4 photochemical cleavage assay of Na^+F21T was also carried out to explore the effects of cation-induced structural changes on photocleavage. The increase in FAM fluorescence as a function of TMPyP4 concentration (Fig. 4B) shows a plateau at TMPyP4 concentration corresponding to a 1-2:1 ratio of TMPyP4 to Na^+F21T. This ratio is lower than that observed K^+F21T (~4:1, see Fig. 4A) presumably reflecting a lower stoichiometry of binding to the Na^+-stabilized quadruplex. In addition, the initial rate of photocleavage of Na^+F21T is greater than that of the K^+F21T. For the Na^+F21T, the solution fluorescence is greater for all samples irradiated for short times (5–30 min) in the presence of TMPyP4 when compared to data for K^+F21T. The only exception is for samples irradiated for 30 min in the presence of the highest TMPyP4 concentration. At longer irradiation times, there is no further increase in fluorescence; instead, there is an apparent decrease of fluorescence at high TMPyP4 concentrations, such that at 120 min, the fluorescence is greater in the case of the K^+F21T.

The photochemical cleavage of F-c-Myc22m-T by TMPyP4 is strikingly different from the photocleavage reactions of either K^+F21T or Na^+F21T (Fig. 4C). The maximum increase in fluorescence of F-c-Myc22m-T is obtained from samples irradiated in the presence of 500–750 nM TMPyP4 (2:1 or 3:1 TMPyP4/quadruplex ratio), depending on irradiation time. At higher TMPyP4 concentrations, the fluorescence decreased markedly, especially at longer irradiation times. The maximal fluorescence increase occurs at 500 nM TMPyP4 and 120 min irradiation and corresponds to ca. 70% cleavage of the dual-labeled oligonucleotide, which is a much more efficient photocleavage than that observed for F21T in either K^+- or Na^+-containing buffers.

The increased efficiency of photochemical cleavage of F-c-Myc22m-T by TMPyP4 may be attributed to the greater affinity of TMPyP4 for the parallel c-Myc G-quadruplex when compared to the mixed- or anti-parallel human telomeric quadruplexes.[35] However, the origin of the marked decrease in normalized fluorescence at higher TMPyP4 concentrations, especially at longer irradiation times was not apparent. Interestingly, it was found that this effect is dependent on the time with which the samples were ex-

posed to TMPyP4 before irradiation (Supplementary data, Fig. S4). Only when irradiation is carried out immediately after addition of TMPyP4 does the apparent cleavage at the higher TMPyP4 concentration exceed that at the lower concentration.

2.2. Oxidative cleavage by Mn·TMPyP4

The oxo-metalloporphyrin Mn(=O)TMPyP4, generated in situ by oxidation of Mn·TMPyP4, has been reported to cleave the G-quadruplex formed by the human telomeric sequence.[29] Thus, in addition to TMPyP4 photochemical cleavage, a study of the oxidative cleavage of G-quadruplex structures by Mn(=O)TMPyP4 was undertaken. As shown in Figure 5A, even at very short reaction times, there is significant apparent cleavage of K^+F21T, as evidenced by increased FAM fluorescence. The maximum fluorescence increase, corresponding to 55% cleavage was found for samples incubated in the presence of 750 nM of Mn·TMPyP4 for 15 min after the addition of oxidant, the longest reaction time employed. At higher Mn·TMPyP4 concentrations, the apparent cleavage determined by FAM fluorescence is reduced. Control reactions in which K^+F21T was incubated with $KHSO_5$ in the absence of Mn·TMPyP4 did not show any changes in FAM fluorescence.

The effect of G-quadruplex DNA structural variations mediated by metal ions on the oxidative cleavage by Mn·TMPyP4 was also investigated. As shown in Figure 5B, when Na^+F21T was subjected to cleavage conditions with increasing concentrations of Mn·TMPyP4 in the presence of $KHSO_5$, the fluorescence increased with increasing reaction time. However, there was very little change in fluorescence with increasing concentration of Mn·TMPyP4 above 250 nM, which corresponds to a 1:1 ratio of metalloporphyrin to G-quadruplex. The maximal increase in fluorescence, corresponding to ca. 30% cleavage of Na^+F21T was observed after 15 min and >250 nM Mn·TMPyP4.

The G-quadruplex formed by F-c-Myc22m-T is a particularly good substrate for oxidative cleavage by Mn·TMPyP4. As shown in Figure 5C, the fluorescence of F-c-Myc22m-T is increased dramatically, even after just 1 min of treatment with 250 nM Mn·TMPyP4 in the presence of $KHSO_5$. The fluorescence increases further with increasing reaction times, but there is little increased fluorescence observed as the Mn·TMPyP4 concentration is increased above 250–500 nM, particularly at the longer reaction times. The maximal increase in fluorescence, corresponding to over 50% cleavage of F-c-Myc22m-T was observed after 15 min in the presence of 500 nM or higher Mn·TMPyP4.

2.3. PAGE analysis

In order to gain additional insight into the G-quadruplex cleavage products, aliquots from selected G-quadruplex cleavage reactions were directly analyzed by PAGE using FAM emission to visualize the gels. In addition, portions of these samples were also first subjected to piperidine/heat treatment prior to PAGE analysis in order to reveal base/heat labile DNA lesions.

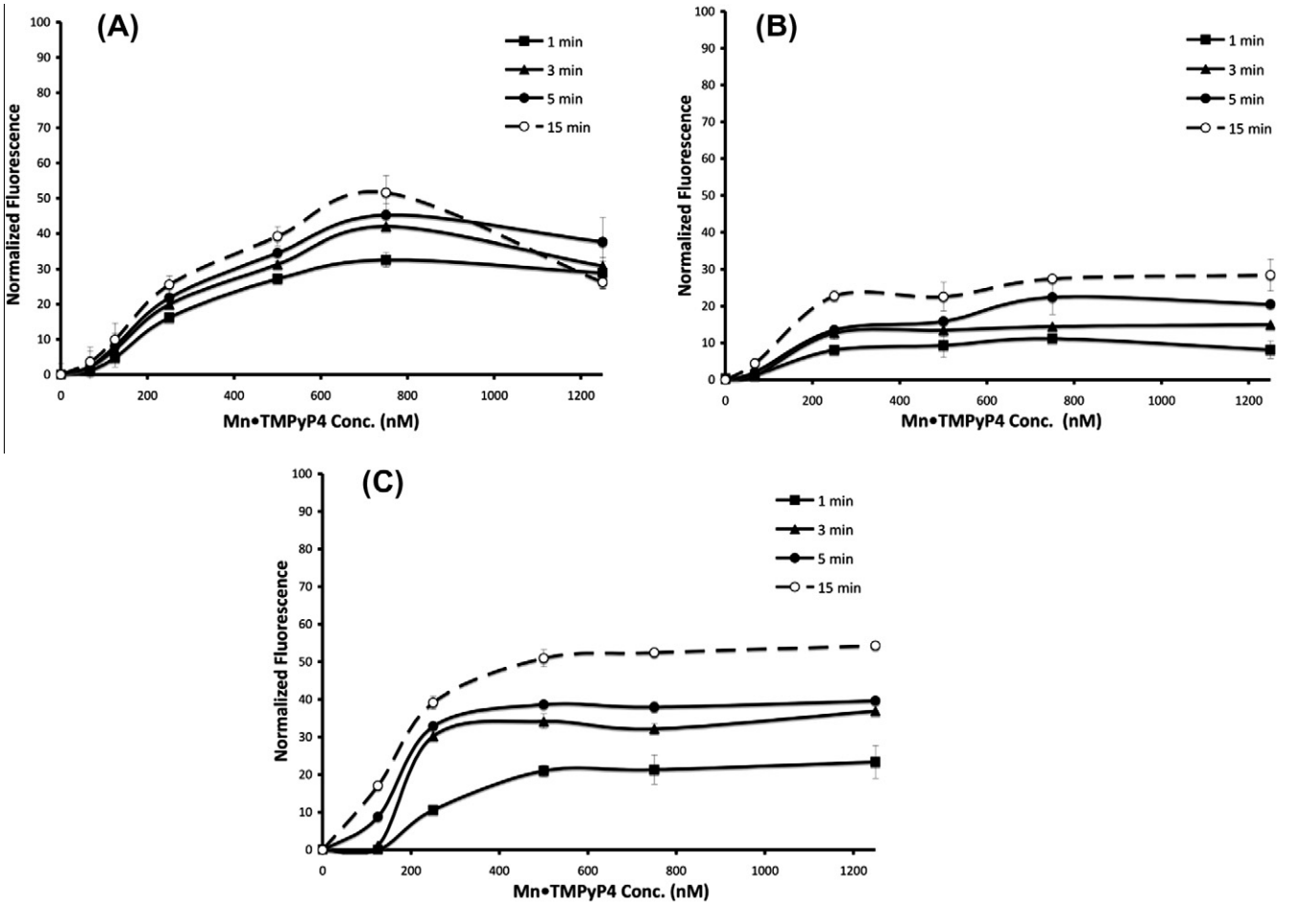

Figure 5. Normalized fluorescence intensity for different G-quadruplex DNA samples (250 nM) subjected to oxidative cleavage for 1–15 min in the presence of 0–1.25 μM Mn·TMPyP4 and $KHSO_5$ (100 μM). (A) K^+F21T (250 nM) in 50 mM potassium cacodylate buffer. (B) Na^+F21T (250 nM) in 50 mM sodium cacodylate buffer. (C) F-c-Myc22m-T in 50 mM potassium cacodylate buffer.

Our previous studies demonstrated the correlation between the extent of G-quadruplex cleavage measured solution fluorescence and the percent DNA cleavage as determined by direct PAGE analysis of samples of K^+F21T treated with hydroxyl radical.[31] To further validate the solution fluorescence assay, samples from the cleavage assays of Na^+F21T and K^+-F21T subjected to photochemical cleavage in the presence of different concentrations of TMPyP4 after 60 and 120 min of irradiation were analyzed by PAGE without prior piperidine/heat treatment. The percent cleavage of the DNA from PAGE analysis shows a strong correlation with the solution normalized fluorescence determined for these samples (r^2 = 0.9195, slope = 1.02, Supplementary data, Fig. S1). These results further demonstrate that the solution fluorescence of these cleavage reactions provides a rapid and accurate measure of the extent of frank G-quadruplex cleavage. However, G-quadruplex lesions that lead to cleavage upon piperidine/heat treatment can be observed by PAGE, but would not be revealed by the solution fluorescence assay. Therefore, to reveal these lesions, selected assay samples were subjected to PAGE analysis both before and after piperidine/heat treatment. The reaction mixtures subjected to PAGE analysis included those that showed only moderate levels of cleavage in the solution fluorescence assay in order to avoid the formation of secondary cleavage products.

Base-labile photochemical lesions are generated on the K^+ F21T G-quadruplex DNA by TMPyP4. When samples were first treated with piperidine and heat prior to electrophoresis, additional G-quadruplex cleavage was evident by the increased intensity of bands corresponding to cleaved products (Fig. 6 right side of gel). There is some cleavage of the 3′-linker and the TAM fluorophore that occurs after piperidine/heat treatment, even in samples that had not been irradiated in the presence of TMPyP4. The bands corresponding to cleavage at the terminal G-tetrads appear much more intense after piperidine/heat treatment. Thus, although photochemical cleavage that does not require base/heat treatment occurs at all G-residues, the base-labile lesions are primarily at the terminal G-tetrads. This preference for photochemical cleavage at terminal G-tetrads is commensurate with that previously reported for TMPyP4 photocleavage of other G-quadruplex structures following piperidine/heat treatment, in which terminal G-tetrads are preferred sites of attack. These sites represent the most favored sites for formation of oxidized G lesions[23] and thus may be due to an electron transfer process for the photocleavage by TMPyP4 that may occur through the G-tetrad stack. Alternatively, the oxidation of these terminal G-residues has been attributed to localized G oxidation in mapping sites of TMPyP4 binding to G-quadruplex structures.[25,26] In contrast, the solution fluorescence signal for photocleavage reactions and cleavage bands observed prior to piperidine/heat treatment from PAGE analysis of these samples, represent a different set of lesions that result in frank strand breakage of the G-quadruplex. These are likely due to hydrogen atom abstraction from the deoxyribose rings, as the resulting radicals can ultimately lead to strand scission without base treatment.[50] Visualization of the gel shown in Figure 6 by TAM fluorescence shows that the 3′-derived DNA cleavage products retain a 5′-phosphate as they co-migrate with Maxam–Gilbert sequencing reaction products (data not shown).

For photochemical cleavage reactions carried out on Na^+F21T, the intensity of the bands corresponding to cleavage of the terminal G-tetrads undergo a less pronounced increase after piperidine/heat treatment when compared to the results from K^+F21T (Supplementary data, Fig. S3). This indicates less efficient electron-transfer mediated photochemical cleavage by TMPyP4 on the Na^+-stabilized G-quadruplex. Thus, TMPyP4 photocleaves K^+F21T quadruplex by direct hydrogen atom abstraction and efficient electron transfer; whereas Na^+F21T is cleaved primarily by hydrogen atom abstraction, possibly due to poorer stacking interactions with terminal G-tetrads of this structure.

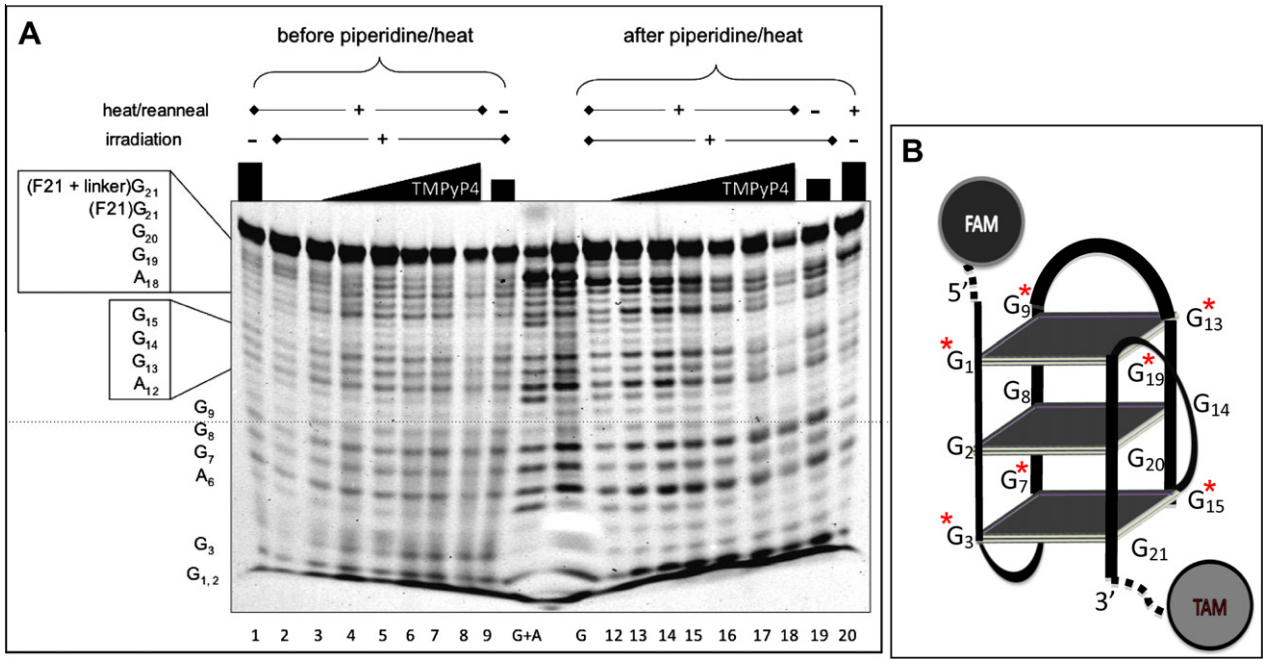

Figure 6. PAGE analysis of G-quadruplex photocleavage reactions of K^+F21T (250 nM) in potassium cacodylate buffer with 0–2.5 μM TMPyP4 irradiated for 30 min (420 nm). Samples in lanes 1–9 were directly subjected to PAGE. Samples in lanes 12–20 were treated with piperidine at 90 °C for 30 min before PAGE analysis. Reactions contained 0 nM (lanes 2, 12), 250 nM (lanes 3, 13), 500 nM (lanes 4, 14), 750 nM (lanes 5, 15), 1000 nM (lanes 6, 16), 1.25 μM (lanes 7, 9, 17, 19), or 2.5 μM (lanes 1, 8, 18, 20) of TMPyP4. Samples in lanes 9 and 19 did not undergo the heat/reanneal cycles. Control samples with TmPyP4 in lanes 1 and 20 were not subjected to irradiation. The gel was visualized by FAM fluorescence. (B) Sites of TMPyP4 photocleavage as determined by PAGE mapped on to the human telomeric (3 + 1) hybrid G-quadruplex structure. Major cleavage sites are marked with a '*'.

PAGE analysis of the TMPyP4 photochemical cleavage reactions of F-c-Myc22m-T demonstrate that the decreased apparent cleavage determined by solution fluorescence at high concentrations of TMPyP4 (Fig. 4C) is not due to changes in the efficiency of quadruplex cleavage, but rather due to photobleaching of the FAM fluorophore. Analysis of the samples subjected to photocleavage by TMPyP4 for 10 min of irradiation by PAGE (Fig. 7A) shows diffuse bands corresponding to cleavage at terminal G tetrads and an intense, fast-moving band corresponding to cleavage of the extreme 5′-end nucleotides. After piperidine/heat treatment all these bands are more intense. There is also evidence for a bias towards cleavage at the 3′ G-tetrad (e.g., G6 > G2; G10 > G8) (Fig. 7B). However, in contrast to the solution fluorescence results (Fig. 4C), the PAGE analysis does not reveal any decrease in G-quadruplex cleavage with increasing TMPyP4 concentration (Supplementary data, Fig. S5).

The oxidative cleavage of F-c-Myc22m-T by Mn·TMPyP4 occurs primarily at G residues. Due to the more rapid cleavage of the c-Myc G-quadruplex by Mn·TMPyP4 as compared to the human telomeric quadruplexes, cleavage reactions of F-c-Myc22m-T in potassium-containing buffer exposed to various concentrations of Mn·TMPyP4 in the presence of $KHSO_5$ for just one min were analyzed by PAGE. As shown in Figure 8, before piperidine/heat treatment, the cleavage products afford diffuse bands that correspond to cleavage at the G17 as well as the penultimate 5′-G run (G8–G10). In addition, low mobility products are also observed in these cleavage reaction mixtures (arrows in Fig. 8A). These low-mobility bands are also seen when the gel is visualized by TAM fluorescence (data not shown), indicating that the products in these bands contain full length DNA, either cross-linked or adducted to the porphyrin. At higher Mn·TMPyP4 concentrations, the intensity of both the higher- and lower-mobility bands increases. After piperidine/heat treatment, PAGE analysis of the F-c-Myc22m-T cleavage products affords more intense and well-resolved bands corresponding to cleavage at G8 and G10. Additional bands are observed corresponding to cleavage at G15 and G19. The intensity of the bands corresponding to cleavage at G17 are not dramatically enhanced after piperidine/heat treatment. Thus, the major lesions formed by Mn(=O)TMPyP4 on the c-Myc G-quadruplex are at specific G residues that map to both G-tetrad faces of the quadruplex (Fig. 8B).

The G-selective cleavage of F-c-Myc22m-T by Mn(=O)TMPyP4 is in contrast to previous reports of cleavage at G residues of a single tetrad and the central T residues in loop regions of human telomeric G-quadruplex substrates.[29] This G-tetrad and T-loop cleavage pattern was also observed upon PAGE analysis of the assay samples from Mn(=O)TMPyP4 cleavage of Na^+F21T and K^+F-21T (Supplementary data, Figs. S6 and S7). In addition, these gels also show low-mobility band corresponding to cross-linked or adducted DNA products, as observed for F-c-Myc22m-T.

2.4. G-quadruplex cleavage selectivity

The solution fluorescence assay can be carried out the presence of unlabeled competitor nucleic acids structures in order to establish the selectivity of various cleavage agents. G-quadruplex cleavage agents that display high affinity to other nucleic acid structures will display diminished G-quadruplex cleavage in the presence of the competitor structure, and the level of this binding selectivity can be related to the concentration of competitor nucleic acid necessary to inhibit G-quadruplex cleavage. For G-quadruplex cleavage agents to be used as probes in complex environments, particularly in cells, this sort of binding selectivity is an important consideration.

Solution fluorescence cleavage assays were carried on F-c-Myc22m-T and K^+F21T (both 250 nM) with TMPyP4 (500 nM) under irradiation or with Mn·TMPyP4 (500 nM) and $KHSO_5$ in the presence of a variety of competitor nucleic acid structures, including G-quadruplex, triplex, duplex, and single-stranded DNA and triplex, duplex, and single-stranded RNA (Fig. 9). As expected, the

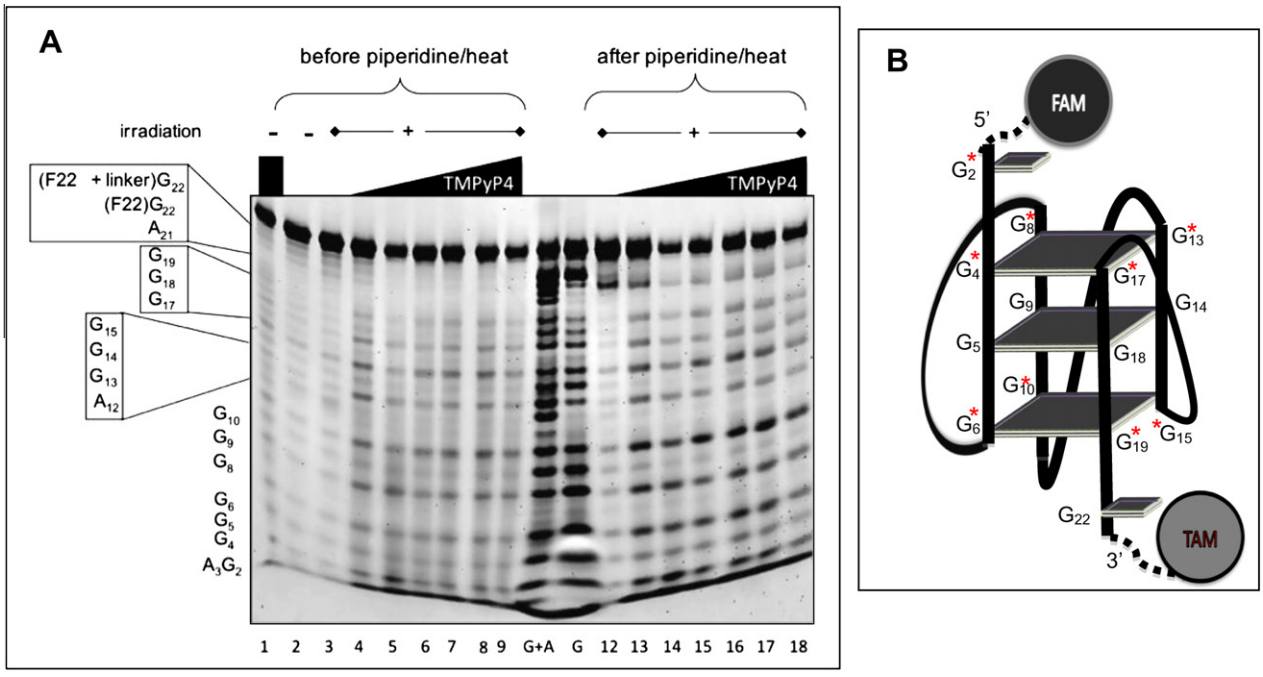

Figure 7. PAGE analysis of G-quadruplex photocleavage reactions of F-c-Myc22m-T (250 nM) in potassium cacodylate buffer with 0–2.5 μM TMPyP4 irradiated for 10 min (420 nm). Samples in lanes 1–9 were directly subjected to PAGE. Samples in lanes 12–20 were treated with piperidine at 90 °C for 30 min before PAGE analysis. Reactions contained 0 nM (lanes 2, 3,12), 250 nM (lanes 4, 13), 500 nM (lanes 5, 14), 750 nM (lanes 6, 15), 1000 nM (lanes 7,16), 1.25 μM (lanes 8, 17), or 2.5 μM (lanes 1, 9, 18) of TMPyP4. Control samples in lanes 1 and 2, with and without TmPyP4 respectively, were not subjected to irradiation. The gel was visualized by FAM fluorescence. (B) Sites of TMPyP4 photocleavage as determined by PAGE mapped on to the c-Myc parallel G-quadruplex structure. Major cleavage sites are marked with a '*'.

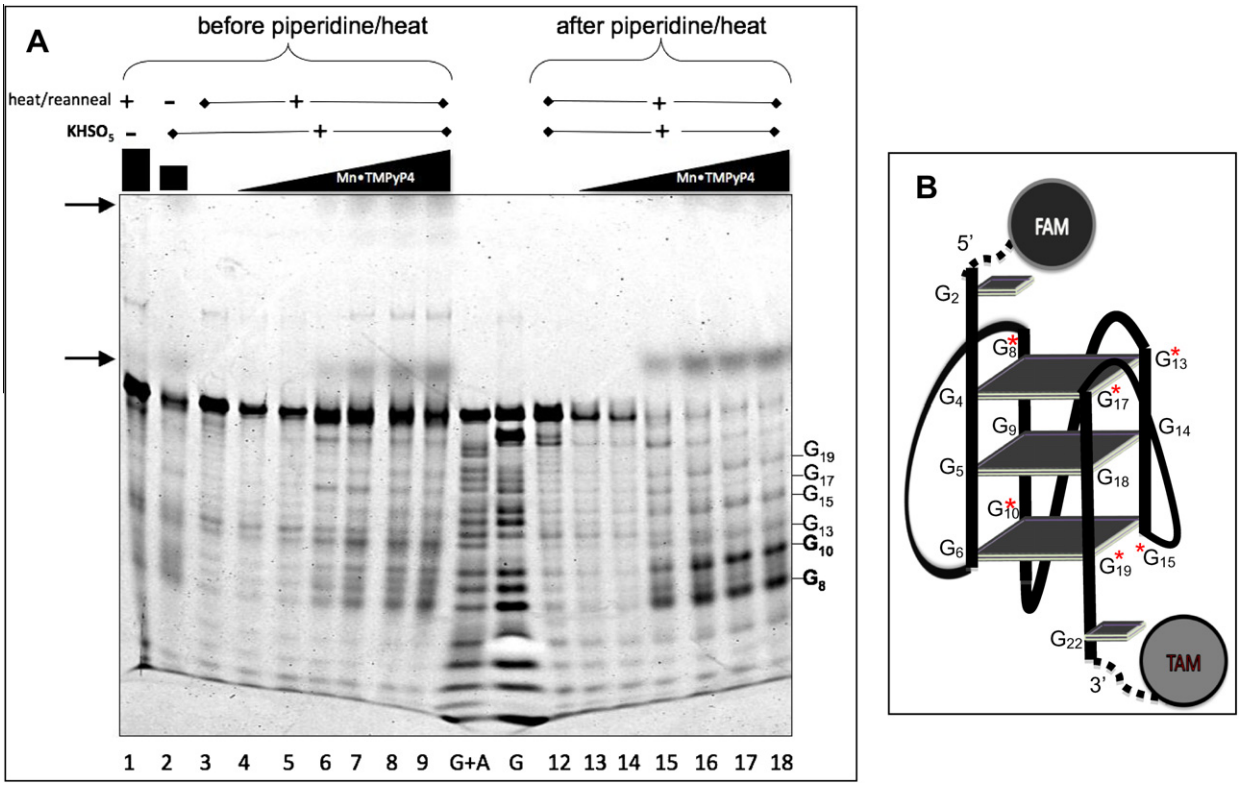

Figure 8. PAGE analysis of G-quadruplex oxidative cleavage reactions of F-c-Myc22m-T (250 nM) in potassium cacodylate buffer with 0–1.25 μM Mn·TMPyP4 and KHSO5 (100 μM) for 1 min. Samples in lanes 1–9 were directly subjected to PAGE. Samples in lanes 12–18 were treated with piperidine at 90 °C for 30 min before PAGE analysis. Reactions contained 0 nM (lanes 3, 12), 67.5 nM (lanes 4, 13), 125 nM (lanes 5, 14), 250 nM (lanes 6, 15), 500 nM (lanes 2, 7, 16), 750 nM (lanes 8, 17) 1.25 μM (lanes1, 9, 18) of Mn·TMPyP4. Control sample not subjected to $KHSO_5$ contained is in lane 1. Sample in lanes 2 did not undergo the heat/reanneal cycle. The gel was visualized by FAM fluorescence. (B) Sites of Mn(=O)TMPyP4 cleavage as determined by PAGE mapped on to the c-Myc parallel G-quadruplex structure. Major cleavage sites are marked with a '*'.

addition of unlabeled c-Myc quadruplex DNA inhibits the cleavage of F-c-Myc22m-T, both in the case of TMPyP4 and Mn(=O)TMPyP4, although the effect is more pronounced for Mn(=O)TMPyP4 (Fig. 9A). This effect is diminished when unlabeled human telomeric G-quadruplex HT is added to F-c-Myc22m-T cleavage reactions, particularly in the case of Mn(=O)TMPyP4. This may reflect the preference for binding to the parallel c-Myc G-quadruplex structure.[34]

Overall, the efficiency of photocleavage by TMPyP4 is more affected by the presence of excess competitor nucleic acids than that of Mn(=O)TMPyP4. This lack of selectivity of TMPyP4 is most pronounced in the case of photocleavage of K^+F21T. Addition of 100-fold excess (relative to K^+F21T) triplex DNA, duplex RNA, and even single-stranded DNA inhibit TMPyP4 photocleavage by >80% (Fig. 9B).

In contrast to the above studies, which measure binding selectivity effects on G-quadruplex cleavage, a more direct means to assess the G-quadruplex cleavage selectivity of these agents was sought. Even G-quadruplex cleavage agents that lack selectivity for binding to G-quadruplex DNA may still cleave these structures preferentially.[61] Thus, we employed solution fluorescence cleavage assays on a dual-labeled duplex hairpin substrate (F-mixed-T) in the same manner as the G-quadruplex cleavage assays, to directly compare the preference for G-quadruplex versus duplex DNA cleavage by these agents.

TMPyP4 photocleaves duplex DNA nearly as efficiently as G-quadruplex DNA. When F-mixed-T is subjected to irradiation in the presence of various concentrations of TMPyP4, there is a marked increase in the normalized FAM fluorescence (Fig. 10A). The maximum normalized fluorescence corresponds to ~40% cleavage at 120 min of irradiation in the presence of 1250 nM TMPyP4 (Fig. 10A). This cleavage efficiency is only slightly less than the 60% and 70% maximal TMPyP4 photocleavage of K^+F21T and F-c-Myc22m-T (Fig. 4A and C), respectively.

Mn·TMPyP4 oxidatively cleaves duplex DNA better than G-quadruplex DNA. When F-mixed-T is subjected to oxidative cleavage in the presence of Mn·TMPyP4, an increase in fluorescence corresponding to 100% cleavage is observed after 15 min, even at 250 nM Mn·TMPyP4, the lowest concentration employed. In contrast, the maximal Mn·TMPyP4 oxidative cleavage of K^+F21T and F-c-Myc22m-T is only 50–55%, and this requires higher concentrations of Mn·TMPyP4 (Fig. 5A and C).

Taken together, these two different means of accessing the binding selectivity and cleavage preference of G-quadruplex by TMPyP4 and Mn·TMPyP4 provide insight to the limitations of these agents and the need for improved selectivity. TMPyP4 displays little preference for G-quadruplex photocleavage, and due to its lack of binding selectivity, its G-quadruplex photocleavage is strongly inhibited in the presence of competitor nucleic acids. Because Mn·TMPyP4 binds more selectively to G-quadruplex DNA, its oxidative cleavage of G-quadruplex structures is less affected by the presence of competitor nucleic acids. However, Mn·TMPyP4 displays a preference towards oxidative cleavage of duplex, rather than G-quadruplex DNA. This may reflect an increased ability of duplex DNA-bound Mn(=O)TMPyP4 to damage DNA compared to the G-quadruplex-bound oxo-metalloporphyrin.

2.5. Identification of a perylene diimide as a G-quadruplex photocleavage agent

Taking advantage of the convenience of the solution fluorescence G-quadruplex cleavage assay, a number of previously re-

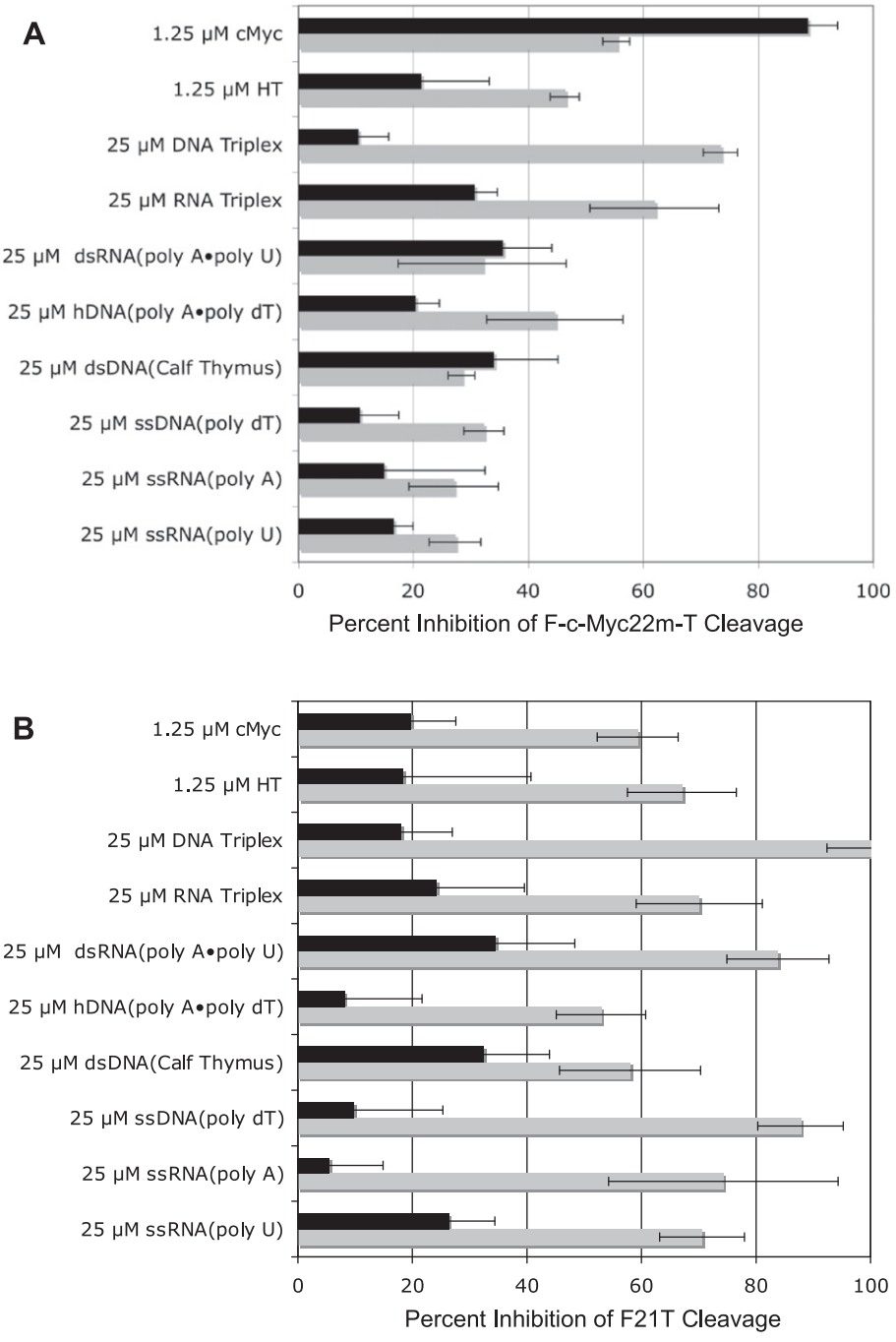

Figure 9. Effect of competitor nucleic acid on the TMPyP4 photochemical (gray bars) and Mn·TMPyP4 oxidative (black bars) cleavage reactions of (A) F-c-Myc22m-T and (B) K^+F21T in 50 mM potassium cacodylate, pH 7.4. Solutions of 250 nM (750 nM tetrad) G-quadruplex DNA (either F-c-Myc22m-T or F21T) with 1.25 or 25 μM competitor (monomeric units) were either irradiated in the presence of 500 nM TMPyP4 for 30 min or subjected to oxidative cleavage with 500 nM Mn·TMPyP4 in the presence of 100 μM $KHSO_5$ for 15 min. After the addition of dissociation buffer (10 μg/well final concentration) and a thermal cycle, the FAM fluorescence of the samples was measured and the percent inhibition of cleavage determined from the normalized fluorescence compared to samples without competitor added.

ported G-quadruplex DNA ligands were screened for their photocleavage ability. This resulted in the identification of Tel11, a 3,4,9,10-perylenetetracarboxylic acid diimide (PDI) as a G-quadruplex selective photocleavage agent. PDI-based G-quadruplex ligands can display high levels of G-quadruplex binding selectivity.[14,51–55] and have been studied as helicase and telomerase inhibitors[53,56] along with their potential to induce telomere damage.[54] However, PDIs have been overlooked as a photocleavage agent despite the well-studied photochemistry of these compounds[56,57] and the known duplex DNA photocleavage by structurally similar naphthalene diimides.[59,60]

As seen in Figure 11A, Tel11 photocleaves F-c-Myc22m-T most efficiently, although all three G-quadruplex structures are cleaved to some extent. The FAM fluorescence of Na^+F21T is increased only when irradiated in the presence of 100 μM Tel11, with the greatest fluorescence increase, corresponding to ~13% cleavage, after 120 min irradiation. K^+F21T displays a more pronounced fluorescence increase, corresponding to ~40% cleavage, in the presence of 100 μM Tel11. In contrast, there is a noticeable increase in fluorescence of F-c-Myc22m-T irradiated in the presence of just 1 μM Tel11. While the largest fluorescence increase of F-c-Myc22m-T, corresponding to ~45% cleavage at 100 μM Tel11, is only slightly

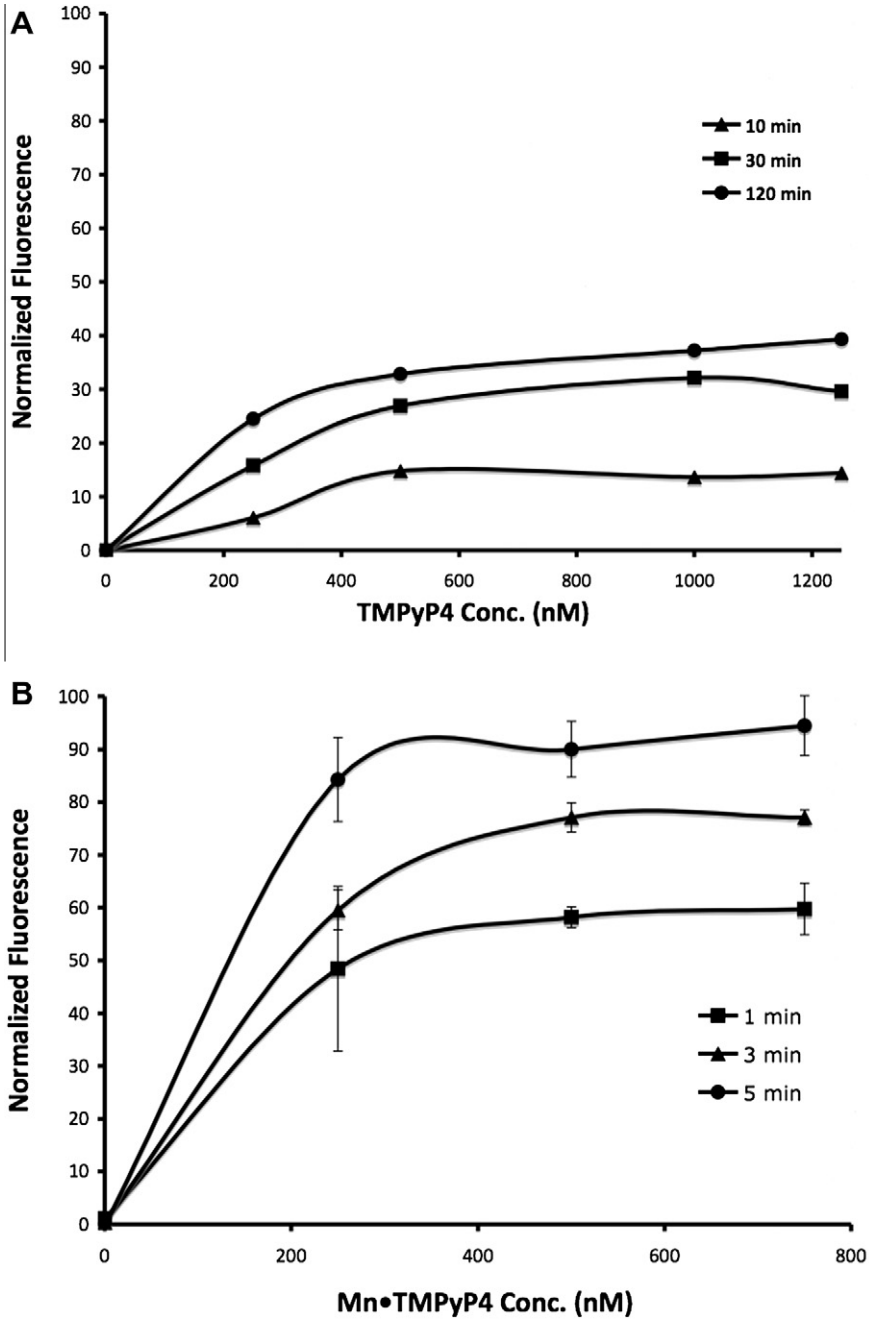

Figure 10. Normalized fluorescence intensity for the duplex hairpin F-mixed-T (250 nM) in 50 mM potassium cacodylate buffer (A) irradiated in the presence of 0–1.25 μM TMPyP4 for 10–120 min by 420 nm lamps. (B) Incubated with 0–750 nM Mn·TmPyP4 in the presence of 100 μM $KHSO_5$ for 1–5 min.

higher than the cleavage of K^+F21T at this Tel11 concentration, significantly more cleavage is observed for F-c-Myc22m-T irradiated in the presence of 10 μM of Tel11 when compared to K^+F21T.

The G-quadruplex DNA photocleavage efficiency of Tel11 is diminished in the presence of excess duplex DNA. As shown in Figure 11A, when the Tel11 photocleavage of F-c-Myc22m-T is carried out in the presence of 100-fold excess (in bp, relative to G-quadruplex) of calf thymus DNA, the fluorescence due to G-quadruplex cleavage is diminished by ~50%. At 10-fold higher competitor duplex DNA concentration, the photocleavage of F-c-Myc22m-T is completely inhibited (data not shown). While direct comparison with the binding selectivity of TMPyP4 and Mn·TMPyP4 is complicated by the higher concentration of Tel11 required for these studies, the inhibitory effect of added duplex DNA on the G-quadruplex photocleavage by Tel11 is in accord with previous studies indicating that Tel11 is a non-selective G-quadruplex DNA binding agent.[52]

Despite the inhibitory effect of duplex DNA on Tel11 photocleavage of G-quadruplex structures, Tel11 has a high preference for cleavage of G-quadruplex versus duplex DNA. When Tel11 photocleavage reactions are carried out on the duplex hairpin F-mixed-T, no significant fluorescence increase is observed, even after 120 min of irradiation in the presence of 100 μM Tel11 (Fig. 11A).

The G-quadruplex photocleavage by Tel11 requires an unsubstituted perylene core. Tel18 is structurally identical to Tel11 with the exception of the perylene bay positions, which are substituted with chlorine atoms in Tel18. Bay position substitution is known to produce a twist in the perylene core, reducing the compound's

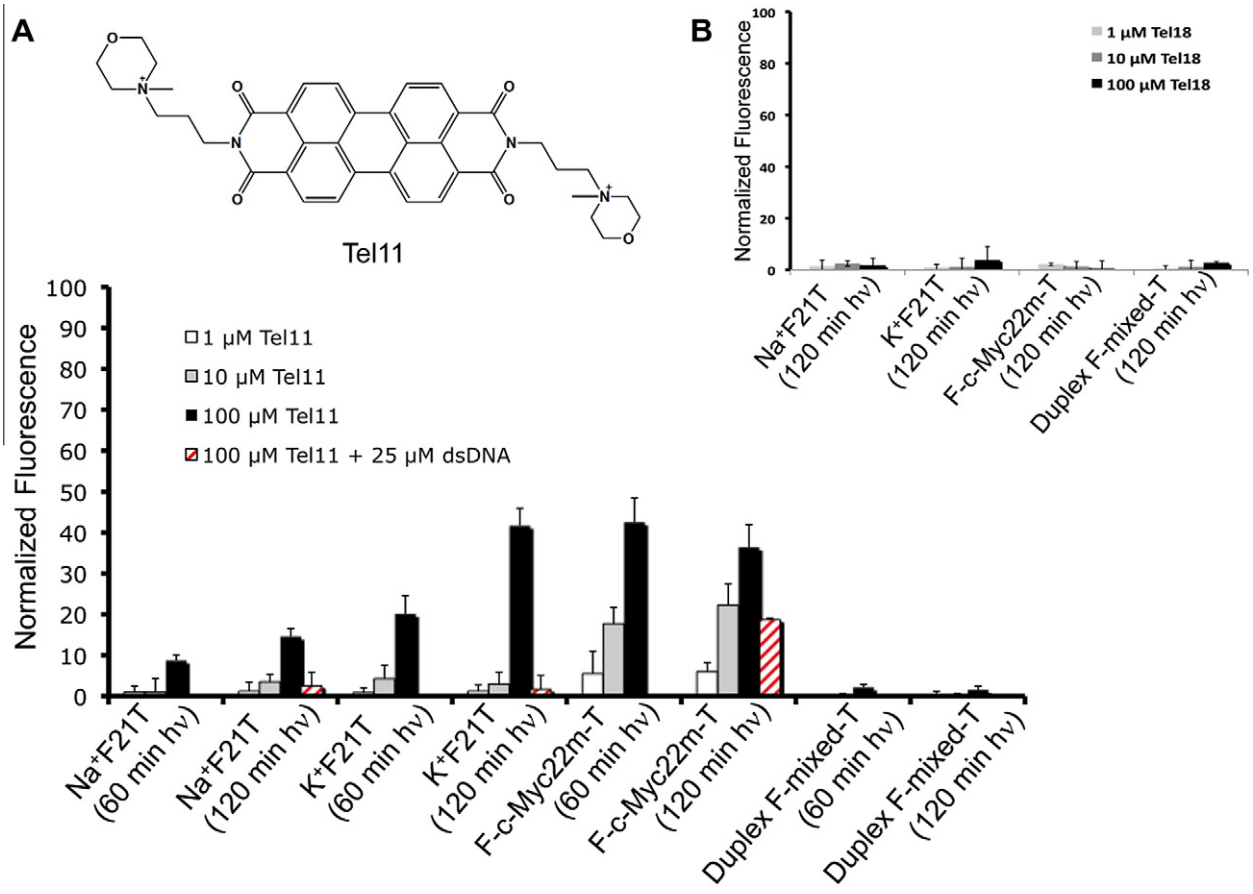

Figure 11. (A) Normalized fluorescence intensity of 250 nM G-quadruplex (K^+F21T, Na+F21T, or F-c-Myc22m-T) or duplex (F-mixed-T) DNA samples irradiated in the presence of 1–100 μM Tel11 for 60 and 120 min by 420 nm lamps in 50 mM potassium or sodium cacodylate buffer. Where indicated 25 μM base-pair duplex calf thymus DNA was also added to the reaction to determine the extent of binding selectivity. (B) Normalized fluorescence intensity of 250 nM G-quadruplex (K^+F21T, Na+F21T, or F-c-Myc22m-T) or duplex (F-mixed-T) DNA samples irradiated for 120 min in the presence of 0–100 μM Tel18.

ability to self aggregate and π stack with DNA.[58] Photocleavage reactions carried out with bay-substituted analog Tel18 did not result in increased fluorescence for any of the substrates under any reaction conditions (Fig. 11B).

PAGE analysis of Tel11 F-c-Myc22m-T photocleavage reactions reveal a distinct cleavage pattern from that observed in either TMPyP4 or Mn·TMPyP4 cleavage of this G-quadruplex. When Tel11 photocleavage reactions were analyzed by PAGE prior to piperidine/heat treatment, bands corresponding to cleavage of the terminal 5′-G (G2) and the 5′-G on each G tract (G4, G8, G13, G17) were observed, especially in the samples that had been irradiated for 120 min in the highest concentrations of Tel11 (Fig. 12A, left side of gel). Additional, weaker bands corresponding to the center G of each G tract were also observed. Analysis of these samples after piperidine/heat treatment revealed more intense bands corresponding to the terminal (G2) and 5′-G tetrad (G4, G8, G13, G17). The bands that migrated with Maxam–Gilbert cleavage sites at the center G of each tetrad that were observed before piperidine/heat treatment are missing after this treatment. Instead, additional bands that migrate slightly slower than the Maxam–Gilbert cleavage products at the 5′-G of each G-tract are observed. This is most clearly seen in the case of G8 (Fig. 12A, right side of gel). These bands may correspond to cleavage products at the 5′-terminal G which retain 3′-modified phosphate (e.g., phosphoglycolaldehyde) products. Mapping of these cleavage sites onto the structure of the c-Myc22m G-quadruplex reveals a 5′ G-tetrad cleavage preference. (Fig. 12B). This, together with the observation of cleavage products that migrate differently than Maxam–Gilbert products, demonstrate that Tel11 photocleavage chemistry is quite distinct from that of the model cleavage agents examined here.

PAGE analysis of Tel11 and Tel18 photocleavage reactions confirm the conclusions derived from the solution fluorescence studies. The ability of Tel11 to photocleave K^+F21T was confirmed by PAGE analysis of the solution fluorescence assay samples (Supplementary data, Fig. S8). Interestingly, PAGE analysis revealed that in addition to cleavage products, irradiation of K^+F21T in the presence of Tel11 affords low mobility bands similar to those observed in the case of Mn(=O)TMPyP4 oxidative cleavage (cf. Fig. 8). As these bands can be visualized by both FAM and TAM fluorescence, they indicate either the formation of Tel11–DNA adducts or Tel11-induced DNA cross-linking. These bands are not observed in Tel11 photocleavage reactions of Na^+F21T (data not shown) or F-c-Myc22m-T (Fig. 12A), indicating the importance of the potassium stabilized F21T topology for adduct/crosslink formation. PAGE analysis was also carried out on the Tel18 photocleavage reaction samples. No cleavage bands were observed, confirming the solution fluorescence results.

3. Conclusions

Using a rapid, fluorescence-based G-quadruplex cleavage assay on three different G-quadruplex structures, the G-quadruplex cleavage selectivity for two model cleavage agents has been determined. Comparisons between G-quadruplex structures demonstrate that some G-quadruplex structures are more susceptible to cleavage than others. Cleavage assays carried out in the presence

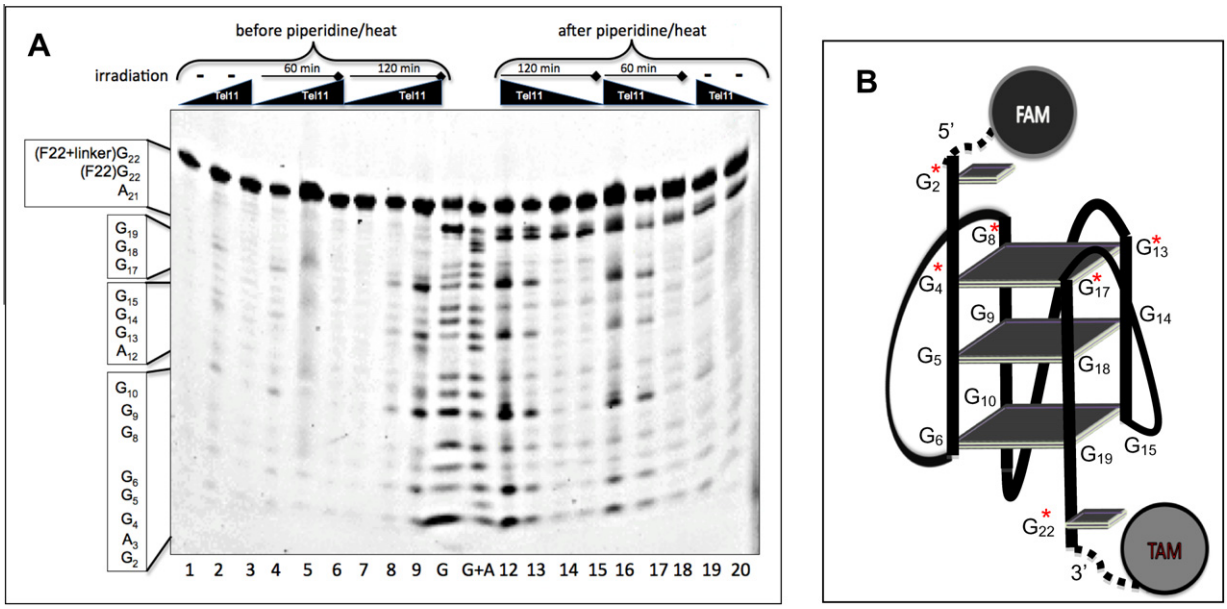

Figure 12. PAGE analysis of G-quadruplex photocleavage reactions of F-c-Myc22m-T (250 nM) in potassium cacodylate buffer with 0–100 μM Tel 11 irradiated for 0–120 min (420 nm). Samples in lanes 1–9 were directly subjected to PAGE. Samples in lanes 12–20 were treated with piperidine at 90 °C for 30 min prior to PAGE. Reactions contained 0 nM (lanes 1, 3, 6, 15, 18, 20) 1 μM (lanes 7, 14), 10 μM (lanes 4, 8, 13, 17) and 100 μM (lanes 2, 5, 9, 12, 16, 19) of Tel 11. Control samples in lanes 1, 2, 19, 20 were not irradiated. Samples in lanes 3–5 and 16–18 were irradiated for 60 min, while those sample in lanes 6–9 and 12–15 were irradiated for 120 min. Maxam–Gilbert sequencing lanes are indicated by the G and G+A. The gel was visualized by FAM fluorescence. (B) Sites of Tel11 photocleavage as determined by PAGE mapped on to the c-Myc parallel G-quadruplex structure. Major cleavage sites are marked with a '*'.

of excess competitor nucleic acid structures reveal the binding selectivity of cleavage agents, while comparisons with direct measurements of duplex cleavage efficiency reveals substrate selectivity for these agents. Finally, the utility of this assay for rapid screening for new G-quadruplex cleavage agents was demonstrated by the identification of the known PDI G-quadruplex ligand Tel11 as a G-quadruplex cleavage agent for the c-Myc promoter structure. These studies are significant because they will facilitate the discovery of novel G-quadruplex cleavage agents targeting specific G-quadruplex structures. These agents may be useful as molecular probes or as therapeutics.

3.1. Selectivity for specific G-quadruplex structures

Of the three G-quadruplex substrates studied here, F-c-Myc22m-T is cleaved most readily by both Mn(=O)TMPyP4 and by photoexcited TMPyP4. In addition, Tel11 was also found to cleave this G-quadruplex best. In all cases, cleavage of F-c-Myc22m-T occurs at terminal G-tetrads, although the specific sites of cleavage and cleavage chemistries for each agent differ. Conversely, Na^+F21T serves as the worse cleavage substrate for all cleavage agents examined. This indicates that parallel-stranded G-quadruplexes such as that formed by c-Myc22m, may serve as particularly good cleavage substrates due to the accessibility of the terminal G-tetrads in these structures when compared to mixed or antiparallel G-quadruplexes, particularly those with transverse loops.

3.2. Cleavage chemistry varies with G-quadruplex structures

One very interesting finding from the PAGE analyses is that for a given cleavage agent, different cleavage products are formed from different G-quadruplex structures. For TMPyP4, more base-labile products are formed from K^+F21T and F-c-Myc22m-T than Na^+F21TT. In the case of Mn(=O)TMPyP4, only G-cleavage is observed with F-c-Myc22m-T, whereas G and T cleavage is seen with Na^+F21T and K^+F21T, although in all three cases there is evidence for adducts or cross-linked DNA products. Adducts were also observed with Tel11, but only in the case of K^+F21T. The precise origin of these changes in cleavage chemistries requires further study, but these results demonstrate that assumptions of unified cleavage mechanisms and products across different G-quadruplex structures can be misleading.

3.3. Selectivity for G-quadruplex cleavage

Utilizing both a direct duplex cleavage assay and G-quadruplex cleavage competitor assay provides a more complete measure of a compound's selectivity and preference for G-quadruplex cleavage than either assay alone. An ideal probe would have a strong preference for cleavage of G-quadruplex substrates versus duplex DNA and have sufficient binding selectivity that the presence of excess competitor nucleic acids, such as duplex DNA, not affect G-quadruplex cleavage. We found that the presence of excess competitor nucleic acid structures most affected the G-quadruplex cleavage for TMPyP4, in accord with the promiscuous nature of this nucleic acid ligand. In contrast, although Mn(=O)TMPyP4 cleavage of G-quadruplex DNA was less affected in the presence of competitor structures, in direct assays of duplex DNA cleavage ability using a dual-labeled hairpin substrate, Mn(=O)TMPyP4 was found to preferentially cleave duplex DNA. Thus, neither of these model agents are very promising as probes. The PDI Tel11 has a higher preference for G-quadruplex versus duplex cleavage than either TMPyP4 or Mn(=O)TMPyP4; however, Tel11 suffers from a lack of G-quadruplex binding selectivity leading to inhibition of G-quadruplex cleavage in the presence of excess duplex DNA.

3.4. Utility of G-quadruplex cleavage assay in screening

The rapid, 96-well format of the fluorescence-based G-quadruplex cleavage assay used here allows screening numerous compounds for cleavage ability. Particularly when carried out in

combination with parallel assays in presence of excess competitor nucleic acids (e.g., duplex DNA), and a break-light assay for duplex cleavage, this assay provides a powerful way to screen for selective G-quadruplex cleavage agents. There are limitations of the assay in terms of the types of lesions that can be detected and potential interference related to the fluors (e.g., photo-bleaching). However, using this assay as a 'front end' in a screening program, with more time-consuming, direct PAGE analysis restricted to the most promising assay samples, has led to the identification of Tel11 as a G-quadruplex cleavage agent. Further studies of the details of the cleavage chemistry of Tel11 and optimization for increased binding selectivity are underway.

4. Experimental section

4.1. DNA purification and tertiary structure formation

The HPLC purified fluorescent dual-labeled oligonucleotides, F21T, (5′-FAM-dGGG(TTAGGG)$_3$-TAM-3′), F-c-Myc22m-T, (5′-FAM-dTGAGGGTGGGTAGGGTGGGTAG-TAM-3′) and hairpin structure F-mixed-T, (5′-FAM-dGCATGCTTTTGCATGC-TAM-3′; FAM: 6-carboxyfluorescein; TAM: tetramethyl-rhodamine) were purchased from Integrated DNA Technologies and used without further purification. The dual-labeled oligonucleotides were diluted from water stock solution to 400 nM in 50 mM sodium or potassium cacodylate, pH 7.4 and annealed by heating to 95 °C for 5 min in a water bath, followed by slowly cooling to room temperature. FRET melting experiments confirmed G-quadruplex formation with melting temperatures of 48, 56 and 85 °C (Na^+F21T, K^+F21T and F-c-Myc22m-T respectively) which correspond closely to the literature values for each G-quadruplex.[40,43,44] The hairpin structure melted at 76 °C, in accord with its theoretical melting temperature. Authentic cleaved F21T, F-c-Myc22m-T and F-mixed-T samples were prepared by incubating 100 pmol of the dual-labeled oligonucleotide with 10 units of S1 nuclease in 10 μL 1× S1 nuclease buffer at 37 °C for 15 min. The reaction was stopped by adding 240 μL of 50 mM potassium cacodylate, pH 7.4. Where indicated, aliquots of these solutions were diluted with the appropriate dissociation buffer and used as an internal standard.

The unlabelled nucleic acid structures used in the competition studies were either synthesized (Expedite 8900) and HPLC purified in-house (HT: dAAA(GGGTTA)$_3$GGGAA), purchased from IDT (c-Myc: dTGAGGGTGGGTAGGGTGGGTAG), purified from commercial calf thymus DNA[62] or prepared from synthetic polynucleotides (Sigma–Aldrich). Triplex structures were prepared by mixing equimolar amounts of its duplex and single strands. Triplex and G-quadruplex structures were annealed by heating to 95 °C for 5 min in a water bath, followed by slowly cooling to room temperature. The structure and purity of these nucleic acid samples were confirmed by UV (Varian Cary Bio 50) and CD (Jasco J-815) spectroscopy. Concentrated stocks were prepared using the monomeric unit of each structure, meaning nucleotides for single strands, base pairs for duplex, triplets for triplex and quartets for quadruplex DNA.[61] The competitor concentrations referenced in these studies refer to these monomeric units.

4.2. Mn·TMPyP4 preparation

Mn·TMPyP4 was prepared from TMPyP4 as described previously.[31,63] Briefly, TMPyP4 chloride (Sigma) (1 mmol) and 16 equiv of $MnCl_2$ (Fisher) were mixed in 5 mL of 3:2 water/methanol with catalytic 2,6-lutidine at room temperature. The reaction was monitored by UV–visible spectroscopy (Varian Cary100) and determined to be complete after 24 h. Excess Mn^{2+} was removed by adding 16 meq of analytical grade Chelex100 resin (sodium salt, BioRad) and stirring for 1 h at room temperature and decanting the supernatant. Metalloporphyrin concentration was determined spectrophotometrically: ε_{462nm} = 101,000 M^{-1} cm^{-1}.[62]

4.3. Photochemical cleavage by TMPyP4

To minimize background cleavage, all manipulations were carried out under subdued lighting. Triplicate 20 μL reaction mixtures of 250 nM of annealed K^+F21T and 0–2.5 μM TMPyP4 tosylate (Sigma) in 50 mM potassium cacodylate, pH 7.4 were placed in a 96-well plate incubated at room temperature in the dark for 30 min. Control wells were blocked from light by a sheet of aluminum foil, and a glass plate was placed over all the wells to filter UV light under 300 nm. The 96 well assay plate was then placed in a Luzchem photoreactor equipped with eight RPR-4190 lamps (emission centered at 420 nm) (Rayonet) for 0–120 min. After irradiation, 180 μL of dissociation buffer (5.55 mM potassium cacodylate, pH 7.4 and either 10 μg/well calf thymus DNA or 2.22% SDS) was added to the wells which were then covered with foil. After the last time point, samples were subjected to thermal denaturation/reannealing as described below. This same method was used for the photochemical cleavage of Na^+F21T in sodium cacodylate buffer and F-c-Myc22m-T and F-mixed-T in potassium cacodylate buffer; however the thermal denaturation/reannealing step was omitted for reactions using F-mixed-T.

4.4. Oxidative Mn·TMPyP4 cleavage

Triplicate reaction mixtures containing 312.5 nM of K^+F21T and 0–1.56 μM Mn·TMPyP4 in 62.5 mM potassium cacodylate, pH 7.4 (16 μL) were placed in individual wells of a 96 well fluorescent plate and preincubated for 30 min at room temperature. Oxidative cleavage reactions were initiated by adding 4 μL of 500 μM $KHSO_5$ (Sigma) freshly prepared in water and stopped after 0–15 min by the addition of 180 μL dissociation buffer (5.55 mM potassium cacodylate pH 7.4 and 10 μg calf thymus DNA/sample). Following the last time point, samples were subjected to thermal denaturation/reannealing as described below. This same method was used for the oxidative cleavage of Na^+F21T in sodium cacodylate buffer and F-c-Myc22m-T and F-mixed-T in potassium cacodylate buffer; however the thermal denaturation/reannealing step was omitted for reactions using F-mixed-T.

4.5. Photochemical cleavage by Tel11 and Tel18

The syntheses of Tel11 and Tel18 were described previously.[14,52] Aside from the concentration range utilized (0–100 μM), the photochemical cleavage reactions by Tel11 and Tel18 were performed as described above for TMPyP4 photochemical cleavage.

4.6. Heat denaturation and reannealing

Separate FRET T_m experiments were first performed to establish the temperature range of stability and to ensure the conditions allowed G-quadruplex reannealing of the intact oligonucleotides in the presence of the dissociation buffer. In order to prevent evaporation during heating/reannealing, the 96-well plates were affixed with an airtight seal (0.05 mm adhesive polyester seal-Uniseal, Whatman). The plates were heated for 30 min in an 85 °C oven and then cooled to room temperature. This specific time and temperature was chosen to ensure complete G-quadruplex denaturation while preventing the thermal distortion of the polystyrene 96-well plates that occurs at more elevated temperatures. After cooling, the plates were spun in a swinging bucket rotor centrifuge

(Eppendorf, 5810R) for 5 min at 3000 rpm to remove condensation on the seal and the seal was carefully removed. After addition of standards to empty wells, the FAM fluorescence was measured and normalized as described below.

4.7. Quantification of cleavage products

The FAM fluorescence of each well was measured five times using a Perkin Elmer Victor 3V plate reader (fluorescence filters: ex 485 ± 13 nm, em 535 ± 25 nm) and the signal averaged FAM emission intensity was corrected for the fluorescence of ligand (if present) to give F_x, average FAM emission of the sample. The normalized fluorescence for each well was calculated according to Eq. 1:

$$\text{Normalized fluorescence} = (F_x - F_{min})/(F_{max} - F_{min}) \times 100 \quad (1)$$

where F_{min} is the average fluorescence of the corresponding sample that had not been irradiated (dark control) or treated with external oxidants; and F_{max} is the average fluorescence of a completely cleaved dual-labeled construct. The average and standard deviation of the normalized solution fluorescence of replicate samples ($n = 3$) is reported. Note: The concentrations, discussed in the text and shown in the Figures, refer to the concentrations employed in the cleavage reactions, not the final concentrations during fluorescence measurement or during preincubation.

4.8. PAGE analysis

Selected reaction samples were also subjected to PAGE analysis either directly or after piperidine/heat treatment. Ethanol precipitation prior to analysis was determined to be unnecessary when calf thymus DNA was used in the dissociation buffer and the final buffer concentration was minimal (10 mM). Where indicated, selective samples were removed prior to the thermal step to determine whether the prolonged heat affected the extent of cleavage. Samples consisting of 1.5–5 pmol of dual-labeled DNA cleavage products were either lyophilized to dryness or subjected to piperidine heat treatment (10% v/v) (Sigma) for 30 min at 90 °C to induce strand scission. Trace piperidine was removed by repeated additions of water and lyophilization. DNA was then resuspended in 1× denaturing buffer (formamide, 5 mM EDTA), heated to 95 °C for 5 min and subjected to electrophoresis on a 20% denaturing polyacrylamide gel (1.5 mm thickness). Standard Maxim–Gilbert sequencing reactions[64] of the dual-labeled oligonucleotides were also loaded on the gel to aid in the identification of bands. The gel was visualized by a Typhoon Trio monitoring the FAM fluorescence and quantified by GelQuant.Net (BiochemLabSolutions). The percent cleavage for each reaction mixture was calculated using Eqs. 2 and 3:

$$FC_x = C_x/Tot_x \quad (2)$$

$$\text{Percent cleavage} = [(FC_x - FC_o)/(1 - FC_o)] \times 100 \quad (3)$$

where FC_x is the raw fraction of cleaved DNA for a given cleavage reaction, C_x is the sum of the integrated band intensity for all cleavage bands in a given lane, Tot_x is the sum of band intensity for all bands in a given lane, and FC_o is the raw fraction of cleaved DNA determined for a control sample not subjected to the cleavage reaction conditions.

4.9. G-quadruplex cleavage in the presence of competitor nucleic acids

Triplicate 20 μL samples of 250 nM K^+F21T or F-c-Myc22m-T and 25 μM (monomeric unit) of a competitor nucleic acid in 50 mM potassium cacodylate pH 7.4 were prepared with either 500 nM TMPyP4 or 10 and 100 μM Tel 11. The samples were incubated in the dark for 30 min prior to irradiation for 30 min (TMPyP4) or 120 min (Tel11) in a photoreactor equipped with eight RPR-4190 lamps (emission centered at 420 nm) (Rayonet). Triplicate 16 μL samples of 312.5 nM F-c-Myc22m-T or K^+F21T and 31.25 μM (monomeric unit) of a nucleic acid in 62.5 mM potassium cacodylate pH 7.4, were prepared with 625 nM Mn·TMPyP4. These samples were preincubated for 30 min prior to initiating oxidative cleavage by the addition of 4 μL freshly prepared 500 μM $KHSO_5$. All reactions were stopped after 15 min by the addition of 180 μL of the calf thymus dissociation buffer, followed by heat denaturation/reannealing. Note: The concentration of competitor nucleic acid discussed in text or in figures represents its monomeric unit concentration in the cleavage reactions, which contained 250 nM (750 nM in G-tetrad concentration) dual labeled oligonucleotide.

The normalized solution fluorescence and percent error (standard deviation) were calculated as before using Eq. 1. The percent inhibition of cleavage was calculated by Eq. 4:

$$\text{Percent inhibition} = [1 - (FC_x - FC_o)] \times 100 \quad (4)$$

Acknowledgments

This work was supported by the Robert Welch Foundation (F-1298), the Center for Molecular and Cellular Toxicology, and the Texas Institute for Drug and Diagnostic Development (TI3D).

Supplementary data

Supplementary data associated with this article can be found, in the online version, at http://dx.doi.org/10.1016/j.bmc.2012.10.017.

References and notes

1. Simonsson, T. *Biol. Chem.* **2001**, *382*, 621.
2. Parkinson, G. N. In *Quadruplex Nucleic Acids*; Neidle, S., Balasubramanian, S., Eds.; The Royal Society of Chemistry: Cambridge, 2006; pp 1–30.
3. Rachwal, P. A.; Brown, T.; Fox, K. R. *Biochemistry* **2007**, *46*, 3036.
4. Maizels, N. *Nat. Struct. Mol. Biol.* **2006**, *13*, 1055.
5. Ou, T. M.; Lu, Y. J.; Tan, J. H.; Huang, Z. S.; Wong, K. Y.; Gu, L. Q. *ChemMedChem* **2008**, *3*, 690.
6. Neidle, S. *FEBS J.* **2010**, *277*, 1118.
7. (a) Rawal, P.; Kummarasetti, V. B. R.; Ravindran, J.; Kumar, N.; Halder, K.; Sharma, R.; Mukerji, M.; Das, S. K.; Chowdhury, S. *Genome Res.* **2006**, *16*, 644; (b) Verma, A.; Yadav, V. K.; Basundra, R.; Kumar, A.; Chowdhury, S. *Nucleic Acids Res.* **2006**, *37*, 4194; (c) Verma, A.; Halder, K.; Halder, R.; Yadav, V. K.; Rawal, P.; Thakur, R. K.; Mohd, F.; Sharma, A.; Chowdhury, S. *J. Med. Chem.* **2008**, *51*, 5641.
8. (a) Siddiqui-Jain, A.; Grand, C. L.; Bearss, D. J.; Hurley, L. H. *Proc. Natl. Acad. Sci. U.S.A.* **2002**, *99*, 11593; (b) Kendrick, S.; Hurley, L. H. *Pure Appl. Chem.* **2010**, *82*, 1609.
9. (a) Huppert, J.; Bugaut, A.; Kumari, S.; Balasubramanian, S. *Nucleic Acids Res.* **2007**, *36*, 6260; (b) Huppert, J. L. *FEBS J.* **2010**, *277*, 3452.
10. Mani, P.; Yadav, V. K.; Das, S. K.; Chowdhury, S. *Plos One* **2009**, *4*, e4399.
11. Nambiar, M.; Goldsmith, G.; Moorthy, B. T.; Lieber, M. R.; Joshi, M. V.; Choudhary, B.; Hosur, R. V.; Raghavan, S. C. *Nucleic Acids Res.* **2011**, *39*, 936.
12. Sissi, C.; Gatto, B.; Palumbo, M. *Biochimie* **2011**, *93*, 1219.
13. Fry, M. *Front. Biosci.* **2007**, *12*, 4336.
14. Tuesuwan, B.; Kern, J. T.; Thomas, P. W.; Rodriguez, M. L.; Li, J.; David, W. M.; Kerwin, S. M. *Biochemistry* **1896**, *2008*, 47.
15. Sun, H.; Yabuki, A.; Maizels, N. *Proc. Natl. Acad. Sci. U.S.A.* **2001**, *98*, 12444.
16. Bashkirov, V. I.; Scherthan, H.; Solinger, J. A.; Buerstedde, J. M.; Heyer, W. D. *J. Cell Biol.* **1997**, *136*, 761.
17. Heller, A. *Faraday Discuss.* **2010**, *116*, 1.
18. Grygoryev, D.; Zimbrick, J. D. *Radiat. Res.* **2010**, *173*, 110.
19. Delaney, S.; Barton, J. K. *Biochemistry* **2004**, *42*, 14159.
20. Ndlebe, T.; Schuster, G. B. *Org. Biomol. Chem.* **2006**, *4*, 4015.
21. Szalai, V. A.; Thorp, H. H. *J. Am. Chem. Soc.* **2000**, *122*, 4524.
22. Pothukuchy, A.; Mazzitelli, C. L.; Rodriguez, M. L.; Tuesuwan, B.; Salazar, M.; Brodbelt, J. S.; Kerwin, S. M. *Biochemistry* **2005**, *44*, 2163.
23. Huang, Y. C.; Cheng, A. K. H.; Yu, H. Z.; Sen, D. *Biochemistry* **2009**, *48*, 6794.
24. Kim, M. Y.; Duan, W. H.; Gleason-Guzman, M.; Hurley, L. H. *J. Med. Chem.* **2003**, *46*, 571.
25. Duan, W. H.; Rangan, A.; Vankayalapati, H.; Kim, M. Y.; Zeng, Q. P.; Sun, D. K.; Han, H. Y.; Fedoroff, O. Y.; Nishioka, D.; Rha, S. Y.; Izbicka, E.; Von Hoff, D. D.; Hurley, L. H. *Mol. Cancer Ther.* **2001**, *1*, 103.

26. Han, F. X. G.; Wheelhouse, R. T.; Hurley, L. H. *J. Am. Chem. Soc.* **1999**, *121*, 3561.
27. Han, H. Y.; Langley, D. R.; Rangan, A.; Hurley, L. H. *J. Am. Chem Soc.* **2001**, *123*, 8902.
28. Tuntiwechapikul, W.; Salazar, M. *Biochemistry* **2001**, *40*, 13652.
29. Vialas, C.; Pratviel, G.; Meunier, B. *Biochemistry* **2000**, *39*, 9514.
30. Zheng, K. W.; Zhang, D.; Zhang, L. X.; Hao, Y. H.; Zhou, X. A.; Tan, Z. *J. Am. Chem. Soc.* **2011**, *133*, 1475.
31. Schoonover, M.; Kerwin, S. M. In *Frontiers in Nucleic Acids ACS Symp. Series*; Sheardy, S., Winkle, S., Eds.; Oxford Univ. Press: Oxford, 2011; Vol. 1082, pp 13–32.
32. Biggins, J. B.; Prudent, J. R.; Marshall, D. J.; Ruppen, M.; Thorson, J. S. *Proc. Natl. Acad. Sci. U.S.A.* **2000**, *97*, 13537.
33. Freyer, M. W.; Buscaglia, R.; Kaplan, K.; Cashman, D.; Hurley, L. H.; Lewis, E. A. *Biophys. J.* **2007**, *92*, 2007.
34. Parkinson, G. N.; Ghosh, R.; Neidle, S. *Biochemistry* **2007**, *46*, 2390.
35. Arora, A.; Maiti, S. *J. Phys. Chem. B.* **2008**, *112*, 8151.
36. Zhang, H. J.; Wang, X. F.; Wang, P.; Ai, X. C.; Zhang, J. P. *Photochem. Photobiol. Sci.* **2008**, *7*, 956.
37. Gabelica, V.; Baker, E. S.; Teulade-Fichou, M. P.; De Pauw, E.; Bowers, M. T. *J. Am. Chem. Soc.* **2007**, *129*, 895.
38. Croke, D. T.; Perrouault, L.; Sari, M. A.; Battioni, J. P.; Mansuy, D.; Helene, C.; Trung, L. D. *J. Photochem. Photobiol. B.* **2006**, *18*, 41.
39. Aoki, K.; Ishikawa, Y.; Oyama, M.; Tomisugi, Y.; Uno, T. *Chem. Pharm. Bull.* **2003**, *51*, 899.
40. Seenisamy, J.; Rezler, E. M.; Powell, T. J.; Tye, D.; Gokhale, V.; Joshi, C. S.; Siddiqui-Jain, A.; Hurley, L. H. *J. Am. Chem. Soc.* **2004**, *126*, 8702.
41. Cogoi, S.; Xodo, L. E. *Nucleic Acids Res.* **2006**, *34*, 2536.
42. Bernadou, J.; Pratviel, G.; Bennis, F.; Girardet, M.; Meunier, B. *Biochemistry* **1989**, *28*, 7268.
43. De Cian, A.; Guittat, L.; Kaiser, M.; Sacca, B.; Amrane, S.; Bourdoncle, A.; Alberti, P.; Teulade-Fichou, M. P.; Lacroix, L.; Mergny, J. L. *Methods* **2007**, *42*, 183.
44. Guyen, B.; Schultes, C. M.; Hazel, P.; Mann, J.; Neidle, S. *Org. Biomol. Chem.* **2004**, *2*, 981.
45. Mergny, J. L.; Maurizot, J. C. *ChemBioChem* **2001**, *2*, 124.
46. Renciuk, D.; Kejnovska, I.; Skolakova, P.; Bednarova, K.; Motlova, J.; Vorlickova, M. *Nucleic Acids Res.* **2009**, *37*, 6625.
47. Ambrus, A.; Chen, D.; Dai, J. X.; Bialis, T.; Jones, R. A.; Yang, D. Z. *Nucleic Acids Res.* **2006**, *34*, 2723.
48. Wang, Y.; Patel, D. J. *Structure* **1993**, *1*, 263.
49. Ambrus, A.; Chen, D.; Dai, J. X.; Jones, R. A.; Yang, D. Z. *Biochemistry* **2005**, *44*, 2048.
50. Kerwin, S. M. In *Radical and Radical Ion Reactivity in Nucleic Acid Chemistry*; Greenberg, M., Ed.; Wiley: New York, 2009; pp 389–419.
51. Pivetta, C.; Lucatello, L.; Krapcho, A. P.; Gatto, B.; Palumbo, M.; Sissi, C. *Bioorg. Med. Chem.* **2008**, *16*, 9331.
52. Kern, J. T.; Kerwin, S. M. *Bioorg. Med. Chem. Lett.* **2002**, *12*, 3395.
53. Franceschin, M.; Lombardo, C. M.; Pascucci, E.; D'Ambrosio, D.; Micheli, E.; Bianco, A.; Ortaggi, G.; Savino, M. *Bioorg. Med. Chem.* **2008**, *16*, 2292.
54. Casagrande, V.; Salvati, E.; Alvino, A.; Bianco, A.; Ciammaichella, A.; D'Angelo, C.; Ginnari-Satriani, L.; Serrilli, A. M.; Iachettini, S.; Leonetti, C.; Neidle, S.; Ortaggi, G.; Porru, M.; Rizzo, A.; Franceschin, M.; Biroccio, A. *J. Med. Chem.* **2011**, *54*, 1140.
55. Rossetti, L.; Franceschin, M.; Bianco, A.; Ortaggi, G.; Savino, M. *Bioorg. Med. Chem. Lett.* **2002**, *12*, 2527.
56. Fedoroff, O. Y.; Salazar, M.; Han, H. Y.; Chemeris, V. V.; Kerwin, S. M.; Hurley, L. H. *Biochemistry* **1998**, *37*, 12367.
57. Zeidan, T. A.; Carmieli, R.; Kelley, R. F.; Wilson, T. M.; Lewis, F. D.; Wasielewski, M. R. *J. Am. Chem. Soc.* **2008**, *130*, 13945.
58. Li, C.; Wonneberger, H. *Adv. Mater.* **2012**, *24*, 613.
59. Rogers, J. E.; Kelly, L. A. *J. Am. Chem. Soc.* **1999**, *121*, 3854.
60. Kawai, K.; Osakada, Y.; Matsutani, E.; Majima, T. *J. Phys. Chem. B.* **2010**, *114*, 10195.
61. An interesting corollary to this involves charge transport through a duplex DNA region to a G-quadruplex, resulting in preferential damage to the quadruplex as described in Refs. 19,20.
62. Ragazzon, P.; Chaires, J. B. *Methods* **2007**, *43*, 313.
63. Borovkov, V. V.; Lintuluoto, J. M.; Inoue, Y. *Synlett* **1999**, 61.
64. Maxam, A. M.; Gilbert, W. *Methods Enzymol.* **1980**, *65*, 499.